

## A novel metaheuristic approach for control of SEPIC converter in a standalone PV system

Dheeban Sembulingam Sankaralingam<sup>1</sup>, Muthu Selvan Balasubramanian Natarajan<sup>2</sup>,  
Maheswari Muthusamy<sup>3</sup>, Sarojini Bagavath Singh<sup>3</sup>

<sup>1</sup>Department of Electrical and Electronics Engineering, Sri Venkateswara College of Engineering Sriperumbudur, Chennai, India

<sup>2</sup>Department of Electrical and Electronics Engineering, Sri Sivasubramaniya Nadar College of Engineering, Chennai, India

<sup>3</sup>Department of Electrical and Electronics Engineering, AAA College of Engineering and Technology Sivakasi, Tamil Nadu, India

### Article Info

#### Article history:

Received Nov 15, 2021

Revised Feb 24, 2022

Accepted Mar 12, 2022

#### Keywords:

Maximum power point tracking

Metaheuristic

PSO

SEPIC converter

Standalone PV

### ABSTRACT

Fossil fuels are being replaced by renewables. Most of the renewables are intermittent, to have reliable power the renewables have to be conditioned before injecting into the utility grid. The DC-DC converters are perfect power electronic devices for conditioning the renewables. The single ended primary inductor converter (SEPIC) performs the conditioning with a very high voltage transfer gain and minimum ripples. The maximum power extraction from the PV panels is required for providing good quality DC power. Intelligent controllers can make use of optimization techniques. The particle swarm optimization (PSO) technique can optimize the controller to extract the maximum power. The SEPIC converter duty variation is optimized and a comparative analysis with the Buck-Boost converter is done in a MATLAB/Simulink environment. The proposed SEPIC converter system performed well by improving the power tracking by 40% and the system has been analysed in a battery charging environment.

*This is an open access article under the [CC BY-SA](https://creativecommons.org/licenses/by-sa/4.0/) license.*



### Corresponding Author:

Dheeban Sembulingam Sankaralingam  
Department of Electrical and Electronics Engineering  
Sri Venkateswara College of Engineering Sriperumbudur  
Chennai, India  
Email: dheebanss@ieee.org

## 1. INTRODUCTION

Renewable energy integration is essential for maintaining the utility grid as pollution-free. The renewable energies that are being mostly wide are solar energy and wind energy. The renewable energy integration can be integrated with the grid to form an on-grid system [1], [2] or an off-grid system [3], [4]. The integrated renewable energy has to be conditioned by a DC-DC converter to ensure high quality of power [5]–[7]. The DC-DC converter is of different topologies and the selection of the DC-DC converter is based on the application [8]. In the applications where negative polarity is used the DC-DC converter has to provide negative output for operation [9]. The two main parameters that have to be considered while designing a DC-DC converter are the minimization of switching losses and improvement of voltage transfer gain. The topologies have been evolving in the recent decade.

The Buck-Boost converter topology is one of the conventional DC-DC converter topologies that is implemented to perform both buck and boost operations. The single ended primary inductor converter (SEPIC) is one of the topologies of the DC-DC converter where the operation of the converter is similar to that of the Buck-Boost converter. SEPIC converter can perform both boost and buck operations as per the application. The number of power switches is reduced in the SEPIC converter topology and reduces the

ripples [10]. The SEPIC converter can operate at a higher duty cycle and maintain a higher voltage transfer gain [11]–[13]. The renewable integration with the SEPIC converter enables to operate in both ON-Grid and Off-Grid. In On-Grid, the power from the distributed energy resources (DER) is conditioned by the SEPIC converter and fed to the utility grid. The recent trends involve designing new topologies by keeping the SEPIC as the base model [14]. The research gap rises in the extraction of maximum power when SEPIC converter is integrated for conditioning of power.

The solar energy integration is in need of a controller for extracting the maximum amount of power even during partial shading conditions. The extraction of power is carried out through Maximum power point tracking (MPPT) controllers [15]–[18]. The MPPT control algorithm has also been evolving throughout the years by embedding with intelligent controllers. The intelligent controllers play an improved role in extracting the maximum power [19]–[21]. The MPPT controller can be made to work more efficiently in varying irradiation by embedding an optimization technique. The particle swarm optimization (PSO) technique has been embedded in the proposed work for maximum power point tracking. The SEPIC converter outputs in the first quadrant that is more suitable for electric vehicle and battery storage applications [22]–[25]. The paper involves a discussion of the operation of the SEPIC converter in section 2 followed by the design of the SEPIC converter. The PV integration with the SEPIC converter has been discussed in section 4 and the optimization technique has been discussed in section 5. The analysis of the system has been done in a MATLAB/Simulink environment and was validated through a hardware prototype.

## 2. SEPIC CONVERTER

The SEPIC converter has power switches like MOSFET ( $Q_{\text{Switch}}$ ) that are suitable for faster switching operations. Two inductors ( $L_{1\_SEPIC}$  and  $L_{2\_SEPIC}$ ), two capacitors ( $C_{1\_SEPIC}$  and  $C_{2\_SEPIC}$ ), and a diode ( $D_{SEPIC}$ ) are used for the operation of the DC-DC converter. The operation of the SEPIC converter depends on the variation of the duty cycle ( $\delta$ ). The duty cycle variation is made to control the switch  $Q_{\text{Switch}}$ . The equivalent circuit of the SEPIC converter is illustrated in Figure 1.

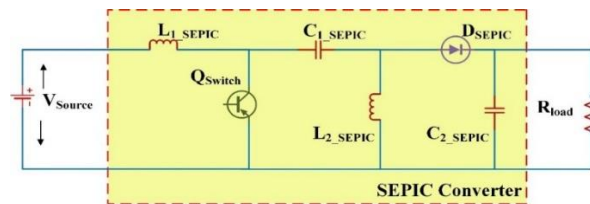


Figure 1. Equivalent circuit of SEPIC converter

Where,

$$\begin{aligned} L_{1\_SEPIC} &= L_{2\_SEPIC} = 2.9\text{mH}, \\ \text{coupling capacitor } C_{pv} &= 220\mu\text{F}, \\ C_{1\_SEPIC} &= 200\mu\text{F}, \\ C_{2\_SEPIC} &= 6600\mu\text{F} \text{ and} \\ R_{Load} &= 32\Omega. \end{aligned}$$

The SEPIC converter has the capability to operate in both continuous conduction mode (CCM) and discontinuous conduction mode (DCM). The differentiation in the operation of CCM and DCM primarily depends upon the energy storage elements like an inductor. The SEPIC converter can buck or boost the input voltage as per the variation in the duty cycle. The energy transfer from the input to the load side is performed by the transfer of energy through various passive elements like inductors and capacitors. Hence the design of inductors and capacitors plays a vital part in the operation of the SEPIC converter. The inductor is selected to handle 40% of the maximum value of input current as ripple current [10]. The ripple current value calculated for both the inductors remains the same. The maximum peak value of the inductors ( $L_{1\_SEPIC}$  and  $L_{2\_SEPIC}$ ) can be enumerated from (1) while the ripple current of the inductors and inductor values can be evaluated from (2) and (3) respectively.

$$I_{L1\_SEPIC\_peak} = I_{Output} * \frac{V_{Output} + V_{D\_SEPIC}}{V_{Input\_min}} * \left( \frac{40\%}{2} + 1 \right)$$

$$\begin{aligned} I_{L2\_SEPIC\_peak} &= I_{Output} * \left( \frac{40\%}{2} + 1 \right) \\ \Delta I_{L\_ripple} &= I_{Input} * 40\% \end{aligned} \quad (1)$$

$$\Delta I_{L\_ripple} = I_{Output} * \frac{V_{Output}}{V_{Input\_min}} * 40\% \quad (2)$$

$$L_{1\_SEPIC} = L_{2\_SEPIC} = \frac{V_{Input\_min}}{\Delta I_{L\_ripple} * f_{switch}} * \delta_{max} \quad (3)$$

The capacitor  $C_{1\_SEPIC}$  used for coupling function depends on the root mean square (RMS) value of the current. Designing the coupling capacitor for a very large value of the RMS current ensures that the SEPIC can be used for low power applications. The coupling capacitor is designed to withstand 1.5 times the input voltage ( $V_{Input}$ ). The ripple voltage of the coupling capacitor  $C_{1\_SEPIC}$  is given in (4) and the RMS current of the capacitor is given in (5).

$$\Delta V_{C1\_SEPIC} = \frac{I_{Output} * \delta_{max}}{C_{1\_SEPIC} * f_{switch}} \quad (4)$$

$$I_{C1\_SEPIC\_RMS} = I_{Output} * \sqrt{\frac{V_{Output} + V_{D\_SEPIC}}{V_{Input\_min}}} \quad (5)$$

The output current experiences very large ripples as the switching action of  $Q_{Switch}$  makes the transfer of energy from input to output. The DC-link capacitor  $C_{2\_SEPIC}$  must handle those heavy ripples. The ripple handling capacity is determined by the root mean square value of the current. The RMS value of the current in the DC link capacitor and the value of the DC link capacitors are given in (6) and (7).

$$I_{C2\_SEPIC\_RMS} = I_{Output} * \sqrt{\frac{V_{Output} + V_{D\_SEPIC}}{V_{Input\_min}}} \quad (6)$$

$$C_{2\_SEPIC} \geq \frac{I_{Output} * \delta}{\Delta V_{ripple} * 0.5 * f_{switch}} \quad (7)$$

The DC-link capacitor  $C_{2\_SEPIC}$  is designed to withstand 1.5 times the output voltage  $V_{Output}$ . The power switch is selected as metal oxide semiconductor field effect transistor (MOSFET) to operate in a higher switching frequency. The MOSFET and Diode are designed to handle a value of summation of input voltage ( $V_{Input}$ ) and output voltage ( $V_{Output}$ ). The peak current handled by the  $Q_{Switch}$  is given by (8). The Root Mean Square handled by the switch and power dissipated in the switch is given in (9) and (10).

$$I_{QSwitch\_peak} = I_{L1\_SEPIC\_peak} + I_{L2\_SEPIC\_peak} \quad (8)$$

$$I_{QSwitch\_RMS} = I_{Output} \sqrt{\frac{(V_{Output} + V_{Input\_min} + V_{D\_SEPIC}) * (V_{Output} + V_{D\_SEPIC})}{V_{Input\_min}^2}} \quad (9)$$

$$P_{QSwitch} = \frac{I_{QSwitch\_RMS}^2 * R_{Drain\_Source\_ON} * \delta_{max} + (V_{Input\_min} + V_{Output}) * I_{QSwitch\_peak} * Q_{Gate\_Drain} * f_{switch}}{I_{Gate}} \quad (10)$$

The power dissipation in the power switch is based on Drain to Source resistance ( $R_{Drain\_Source\_ON}$ ), the charge from Gate to Drain ( $Q_{Gate\_Drain}$ ), switching frequency ( $f_{switch}$ ), duty cycle ( $\delta$ ), and RMS current and peak current through the switch ( $I_{QSwitch\_peak}$  and  $I_{QSwitch\_RMS}$ ).

### 3. PV INTEGRATED SEPIC CONVERTER

Solar energy is used in place of the input voltage as solar produces clean pollution-free DC output. Solar energy can be used in various topologies. Standalone systems perform effectively in remote and low-power applications. The Photovoltaic cells generated DC current as the cells are being exposed to Sun. The generated current from the PV panels and the design parameters has been discussed in [4]. The generated current from the PV panels is based on the configuration of the PV panel design. The PV panel integrated with the SEPIC converter is shown in Figure 2.

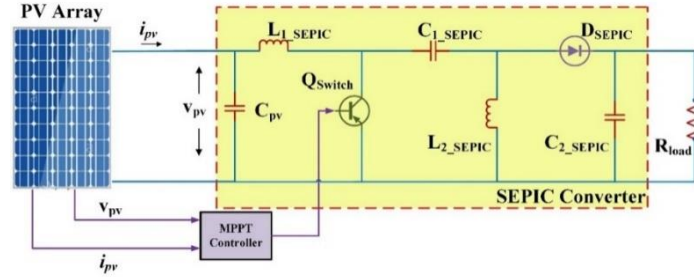


Figure 2. Equivalent circuit of SEPIC converter integrated with photovoltaic panel

The PV panel charges the input capacitor  $C_{pv}$  that limits the variation in change in voltage. The presence of an inductor ( $L_{1\_SEPIC}$ ) makes continuous and triangular input waveform. The capacitor faces a minimum ripple due to the presence of an inductor. The RMS value of current handled by the input coupling capacitor is given in (11).

$$I_{C_{pv\_RMS}} = \frac{\Delta I_{L\_ripple}}{\sqrt{12}} \quad (11)$$

The impedance interaction at the input side can be eliminated by the proper design of the input coupling capacitor. The power and the voltage generated from the photovoltaic panels are intermittent. The PV and IV curves are used for characterizing the PV panels. Hence a constant maximum power capturing system is required for identifying the maximum power point. The voltage ( $v_{pv}$ ) and the current ( $i_{pv}$ ) from the PV panels are sensed from the PV panels and fed to the MPPT controller. The MPPT controller embeds the algorithm to track down the maximum power from the PV panels. The duty cycle ( $\delta$ ) variation is handled by the MPPT controller.

#### 4. MPPT CONTROLLER WITH META-HEURISTIC

The MPPT controller is embedded with an optimization technique to optimize and ensures the tracking is done in a more effective way. The optimization technique used is PSO technique the follows the nature of birds. The nature of PSO optimization works on the positioning of the particles. The present position of the particle ( $m_i^t$ ) is affected by the neighboring particle that is inferred from (12).

$$m_i^{t+1} = m_i^t + v_i^{t+1} \quad i=1,2,3\dots N \quad (12)$$

The velocity of the particle ( $v_i$ ) is an essential parameter for determining the position of the neighboring particle. The best solution from the entire group is to be identified ( $b_{best}$ ) along with its position ( $a_{best}$ ). The velocity of the particle is determined from (13).

$$v_i^{t+1} = c_1 u_1 (a_{best}, i - m_i^t) + (b_{best} - m_i^t) c_2 u_2 + w v_i^t \quad i=1, 2, \dots, N \quad (13)$$

The value of  $u_1$  and  $u_2$  represents the random function that has been uniformly distributed from 0 to 1. The cognitive and social coefficient of the group is represented by  $c_1$  and  $c_2$  respectively. Figure 3(a) determines the particle movement during the process of optimization. The flow chart corresponding to the MPPT duty cycle variation through PSO optimization is illustrated in Figure 3(b).

In the proposed system the PSO optimization is embedded at the MPPT controller. The voltage and current are sensed from the PV panel as the power from the PV panels is considered as the parameter to be optimized. The swarm size is initialized along with PSO constants ( $w$ ,  $c_1$ ,  $c_2$ ) and number of iterations. The fitness is evaluated for each of the particle. Each particle fitness value is evaluated. Through the fitness value, the global fitness value is calculated. The position and velocity of the particle are periodically updated until best optimized outcome. The fitness value is been constantly replaced. The particle's best position and the best solution are verified periodically to optimize the power. The power value obtained through the current and voltage is optimized via the PSO algorithm. The duty cycle is estimated through optimization and given as input to the gate of the power switch.

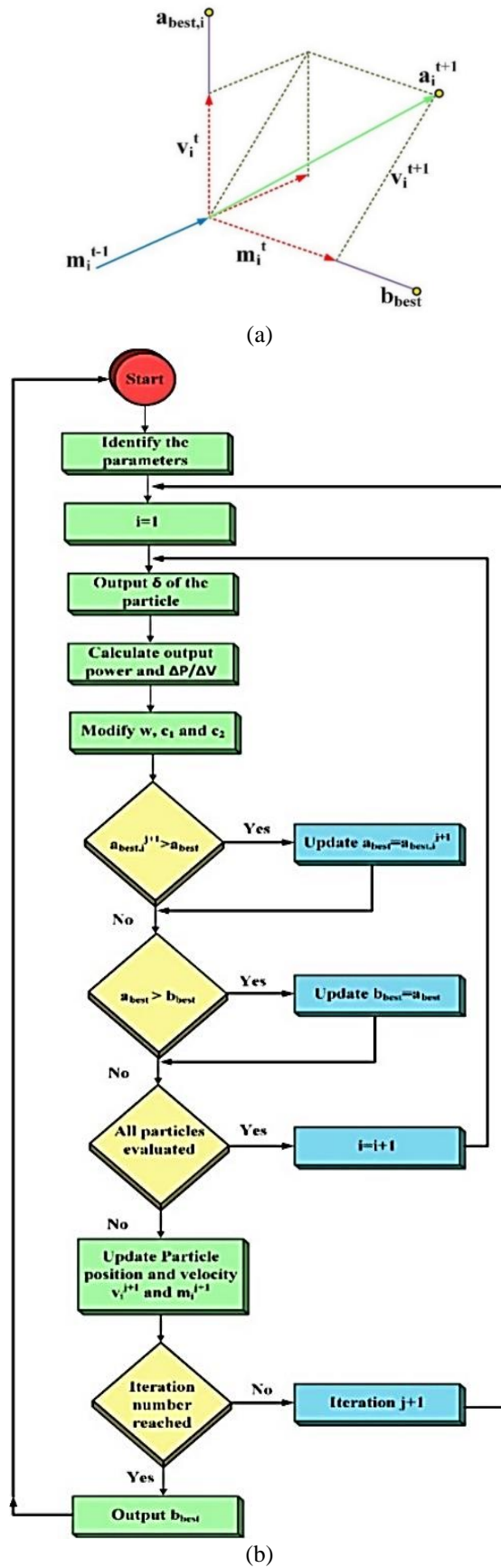


Figure 3. PSO Optimization for MPPT controller (a) position tracking (b) flowchart

**5. RESULTS AND DISCUSSION**

The proposed system of the SEPIC converter was designed and simulated in a MATLAB/Simulink environment. The SEPIC converter input is from a PV array which is designed to produce an output voltage of 22 V. The SEPIC converter parameters are enclosed in the Appendix section. The system was simulated and studied under various conditions.

**5.1. Case 1: PV panel characteristic study**

The parameters of the PV module are given in Table 1 while the I-V characteristics of the PV array is shown in Figure 4(a) and P-V characteristics of the PV array is shown in Figure 4(b). The PV modules are connected in the desired pattern to generate the required voltage and current. The series connection involves connecting 6 modules in series for a string and the parallel connection involves connecting 2 modules. A voltage of 22.2 V and a current of 10.4 A are generated as per the configuration. The system is tested under a varying irradiation pattern from 500 W/m<sup>2</sup> to 1000 W/m<sup>2</sup>. The varying irradiation signal is illustrated in Figure 5(a) and the output voltage obtained during varying irradiation is shown in Figure 5(b). The output voltage from the PV panel varies as per the irradiation to which the is PV panels are being exposed. The output voltage from the PV panel is shown in Figure 5(b). The PV panel output varies corresponding to the exposure of the PV panels to the sunlight. Hence the maximum power is extracted only when the PV panels are exposed to a higher irradiation level.

Table 1. Parameters of PV module

PV module specification	Value
Maximum power (Watts)	14.24 W
No. of cells per module	6
Open circuit voltage (Voltage)	3.7 V
Short circuit current (Ampere)	5.2 A
Maximum power point voltage (Voltage)	2.9 V
Maximum power point current (Ampere)	4.91 A

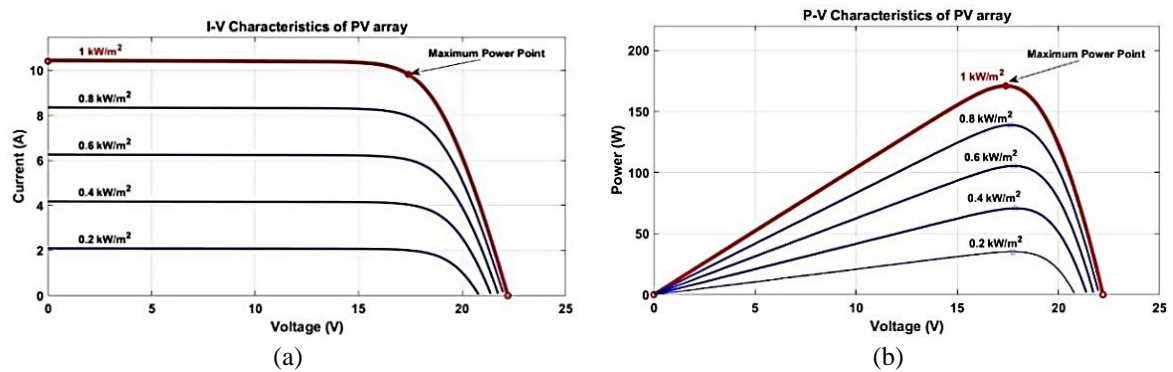


Figure 4. PV array (a) I-V characteristics and (b) P-V characteristics

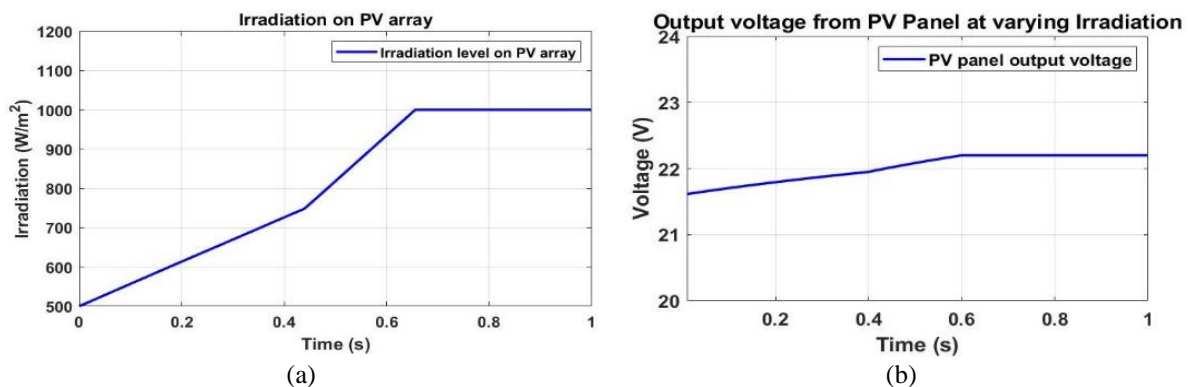


Figure 5. PV panel (a) exposed to varying irradiation and (b) output voltage

### 5.2. Case 2: Comparison of DC-DC converters in standalone PV system

The output from the PV panels is fed to the load through the SEPIC converter. The SEPIC converter conditions the output from the PV panel. The system was also compared with the traditional Buck-Boost converter. The difference between the Buck-Boost converter and SEPIC converter is the operation the Buck-Boost converter outputs a negative value when the polarity of the converter is reversed. But the SEPIC converter outputs a positive voltage even when the polarity is reversed. The SEPIC converter output is positive even at the time of reversal of polarity. The Buck-Boost converter performs the same operation but the output voltage is reversed and also the Buck-Boost converter requires two switches for its control. The SEPIC converter is more suitable for the application of battery charging as it eliminates the shift in polarity. The reason for the SEPIC converter to excel the Buck-Boost in battery charging is the availability and controllability of the power switches. The SEPIC requires a single power switch that reduces the switching time duration when compared with the Buck-Boost. Hence SEPIC converters are mostly used in battery applications like mobile charging and electric vehicles.

### 5.3. Case 3: MPPT controller with meta-heuristic optimization

The MPPT optimization carried out with particle swarm optimization (PSO) is analysed. The MPPT Controller controls the duty cycle for the power switch of the SEPIC converter. The comparative analysis after implementation of PSO technique is shown in Table 2.

The power tracking was effectively improved after optimizing with PSO optimization that can be inferred from Figure 6(a). The output voltage improvement after implementation of the PSO technique is shown in Figure 6(b). The current generation is improved by the optimization of the MPPT controller through PSO technique. The average value of improved power tracking by using the PSO optimization technique is increased by 40%.

Table 2. Difference in the system after implementation with PSO

Duty cycle	Output without PSO technique		Output with PSO technique	
	Voltage (V)	Power (P)	Voltage (V)	Power (P)
10	0.43	0.01	1.37	0.11
20	1.97	0.33	2.84	0.60
30	8.49	3.31	14.51	6.53
40	13.12	7.35	19.77	14.63
50	20.59	14.21	27.48	22.26
60	29.90	26.01	33.63	32.96
70	39.78	49.33	43.49	60.45
80	45.21	64.20	47.83	71.75

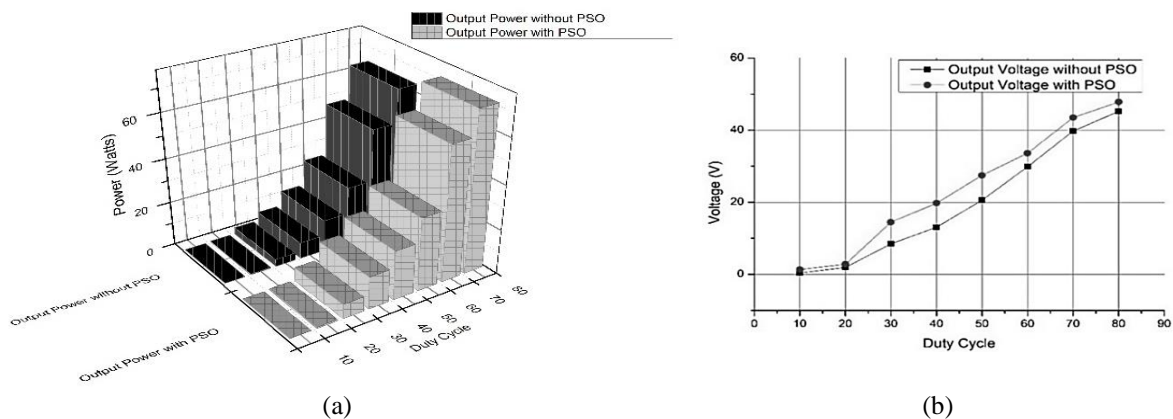


Figure 6. Comparison of (a) power and (b) voltage across duty cycle variation

### 5.4. Case 4: Hardware prototype n

A prototype of SEPIC converter with PSO algorithm embedded for maximum power point tracking was made for an input voltage of 12 V. The SEPIC converter operates to boost the input voltage to 24 V. The specification of the PV panel is given in Table 3. The hardware prototype of the system is shown in Figure 7(a) and Figure 7(b). The power switch selected for the prototype is a MOSFET IRF840N, which provides faster

switching at a very high frequency. The switching frequency used for the purpose is of 1 kHz. The load used for the prototype is a 10 W resistive load. The usage of two inductors separately makes a drop in the efficiency of the converter. The drawback due to the two separate inductors are overcome by coupling the inductor together. The coupling process reduces the current ripples as the inductor size reduces drastically. The microcontroller unit used is a Ds-Pic microcontroller that embeds the program for duty cycle variation. The PSO optimization technique is embedded in the above microcontroller unit. The system was tested for varying irradiation and the output voltage from the PV panel at the time of varying irradiation is shown in Figure 8 for a period of 50  $\mu$ s. The output obtained before PSO optimization is shown in Figure 9(a) and after PSO optimization is shown in Figure 9(b) for a period of 50  $\mu$ s.

Table 3. Hardware PV panel specification

Hardware PV panel specification	Value
Rated power (Watts)	10 W
Rate voltage (Voltage)	17 V
Maximum current (Ampere)	0.57 A
Open circuit voltage (Voltage)	21 V
Short circuit current (Ampere)	0.69 A

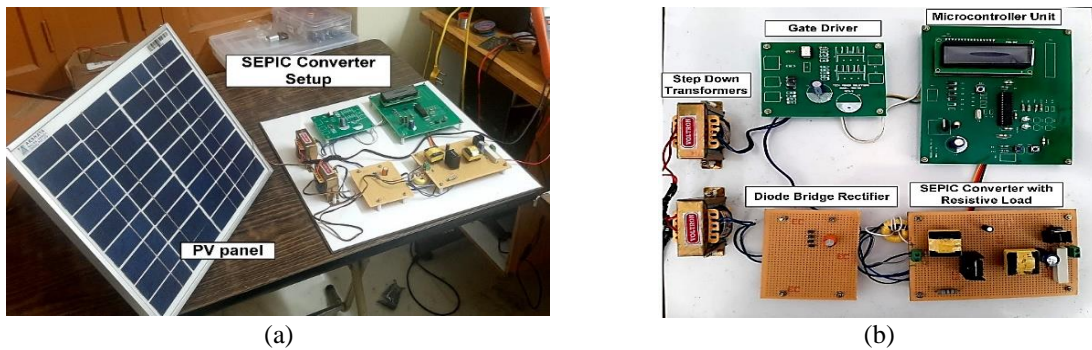


Figure 7. PV integrated SEPIC converter (a) overall hardware setup with PV panel and (b) SEPIC converter setup

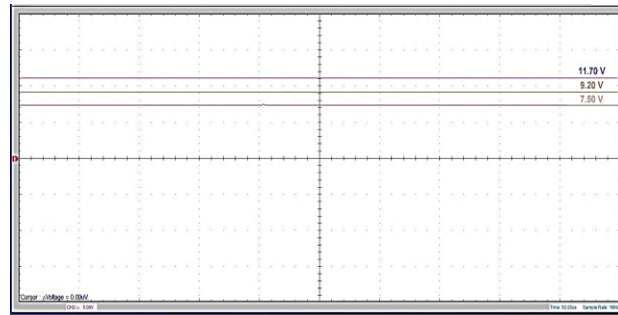


Figure 8. PV panel output during varying Irradiation

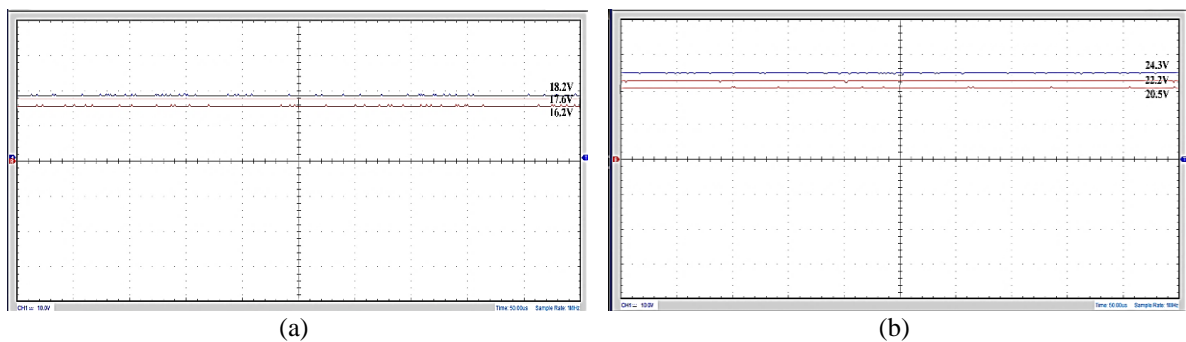


Figure 9. Output voltage obtained (a) without PSO optimization and (b) with PSO optimization

The solar panel is intermittent as the irradiation over the PV panels varies, the output voltage also varies which is evident. The irradiation is varied with respect to three levels contributing to the voltage of 7.5 V, 9.20 V and 11.7 V. The output of the SEPIC converter without PSO technique is observed at various irradiation conditions. The results obtained from the previous analysis is compared along with the results of SEPIC converter operation with PSO technique. The observed voltage under both the conditions is shown in Figure 10 and tabulated in Table 4.

The percentage of output voltage increase proves that the optimized algorithm is more efficient in increasing the voltage gain by an average of 21%. The comparative analysis from Figure 10 illustrates that the optimized algorithm proved an effective power tracking mechanism. The optimized technique was able to extract a maximum value of power from the PV panel and the power was conditioned by the SEPIC converter effectively.

Table 4. Output voltage comparison with PSO technique in SEPIC converter

PV output voltage (V)	SEPIC Converter Output Voltage (V)		Increase in voltage (%)
	Without PSO	With PSO	
7.50	16.20	20.50	20.98
9.20	17.60	22.20	20.72
11.70	18.20	24.30	25.10

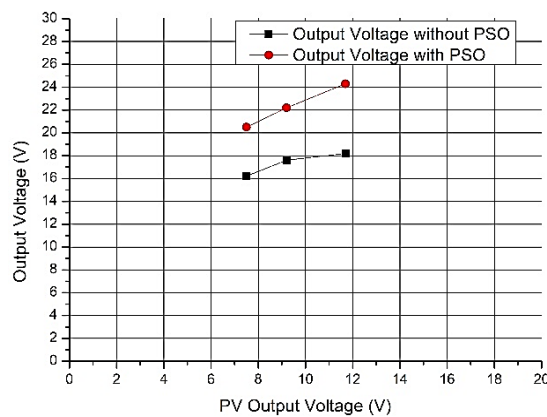


Figure 10. Comparison of hardware SEPIC converter output voltage under PSO optimization

## 6. CONCLUSION

The increase in renewable energy integration like solar and wind energy to the utility grid raises a necessity for proper power conditioning. The power conditioning is carried out through the DC-DC converters. The SEPIC converter can boost or buck the voltage level based upon the application. The SEPIC converter is one of the refined topologies of the buck-boost converter. The SEPIC has a very good response period and has a minimum number of power switches compared to the buck-boost topology. SEPIC finds the specific application over battery charging circuits in EV and mobile charging devices. As these applications are in need of positive polarity of voltage rather than negative, SEPIC outputs the voltage only at the first quadrant. The integration of PV with SEPIC increases the reliability to work in a standalone configuration. The standalone configuration finds more applications in remote areas. The PV power extracted is maximized through power point tracking controllers. The controller is optimized through metaheuristic optimization techniques like PSO. Optimization proved to be an effective method to extract maximum power. The power conditioning of solar energy has been performed by the SEPIC converter along with the optimization technique more efficiently.

## ACKNOWLEDGEMENTS

The authors thank the Principal and Management of Sri Sivasubramaniya Nadar College of Engineering Chennai and Sri Venkateswara College of Engineering Sriperumbudur Chennai for supporting and encouraging them to do this research work. The authors also thank AAA College of Engineering and Technology Sivakasi.

## REFERENCES

- [1] J. Hashimoto, T. S. Ustun, M. Suzuki, S. Sugahara, M. Hasegawa and K. Otani, "Advanced Grid Integration Test Platform for Increased Distributed Renewable Energy Penetration in Smart Grids," in *IEEE Access*, vol. 9, pp. 34040-34053, 2021, doi: 10.1109/ACCESS.2021.3061731.
- [2] D. S. Sankaralingam and V. Kamaraj, "Grid integration of 10kW solar panel," *2016 3rd International Conference on Electrical Energy Systems (ICEES)*, 2016, pp. 257-266, doi: 10.1109/ICEES.2016.7510650.
- [3] D. Bhule, S. Jain and S. Ghosh, "Power Management Control Strategy for PV-Battery Standalone System," *2020 IEEE 9th Power India International Conference (PIICON)*, 2020, pp. 1-6, doi: 10.1109/PIICON49524.2020.9112970.
- [4] K. Dubey and M. T. Shah, "Design and simulation of Solar PV system," *2016 International Conference on Automatic Control and Dynamic Optimization Techniques (ICACDOT)*, 2016, pp. 568-573, doi: 10.1109/ICACDOT.2016.7877649.
- [5] D. S. Sankaralingam and M. S. B. Natarajan, "ANFIS-based Power Quality Improvement by Photovoltaic Integrated UPQC at Distribution System," *IETE Journal of Research*, 2021, doi: 10.1080/03772063.2021.1888325.
- [6] D. S. Sankaralingam, M. S. B. Natarajan, and U. Subramaniam, "Artificial Neural Network based Solar Energy Integrated Unified Power Quality Conditioner," *Energy Sources, Part A: Recovery, Utilization, and Environmental Effects*, 2021, doi: 10.1080/15567036.2021.1919247.
- [7] N. Hou and Y. W. Li, "Family of Hybrid DC-DC Converters for Connecting DC Current Bus and DC Voltage Bus," *2020 IEEE Energy Conversion Congress and Exposition (ECCE)*, 2020, pp. 412-417, doi: 10.1109/ECCE44975.2020.9235473.
- [8] J. D. Navamani, K. Vijayakumar, and R. Jegatheesan, "Reliability and performance analysis of a high step-up DC-DC converter with a coupled inductor for standalone PV application," *International Journal of Ambient Energy*, vol. 41, no. 12, 1327-1335, 2020, doi: 10.1080/01430750.2018.1517662.
- [9] D. S. Sankaralingam, M. S. B. Natarajan and U. Subramaniam, "Power conditioning of standalone Photo-voltaic system with BLDC motor by Negative-Output Luo Converter," *2020 International Conference on Power Electronics and Renewable Energy Applications (PEREA)*, 2020, pp. 1-6, doi: 10.1109/PEREA51218.2020.9339815.
- [10] Z. Zhang, J. Lin, Y. Zhou and X. Ren, "Analysis and Decoupling Design of a 30 MHz Resonant SEPIC Converter," in *IEEE Transactions on Power Electronics*, vol. 31, no. 6, pp. 4536-4548, June 2016, doi: 10.1109/TPEL.2015.2472479.
- [11] E. Babaei and M. E. Seyed Mahmoodieh, "Calculation of Output Voltage Ripple and Design Considerations of SEPIC Converter," in *IEEE Transactions on Industrial Electronics*, vol. 61, no. 3, pp. 1213-1222, March 2014, doi: 10.1109/TIE.2013.2262748.
- [12] M. A. Al-Saffar, E. H. Ismail, A. J. Sabzali and A. A. Fardoun, "An Improved Topology of SEPIC Converter with Reduced Output Voltage Ripple," in *IEEE Transactions on Power Electronics*, vol. 23, no. 5, pp. 2377-2386, Sept. 2008, doi: 10.1109/TPEL.2008.2001916.
- [13] M. Zhu, F. L. Luo and Y. He, "Remaining Inductor Current Phenomena of Complex DC-DC Converters in Discontinuous Conduction Mode: General Concepts and Case Study," in *IEEE Transactions on Power Electronics*, vol. 23, no. 2, pp. 1014-1019, March 2008, doi: 10.1109/TPEL.2008.917956.
- [14] R. Kumari, M. Pandit, and K. S. Sherpa, "Modelling and Comparison of Conventional SEPIC Converter with Cascaded Boost-SEPIC Converter," *Journal of The Institution of Engineers (India): Series B*, vol. 102, no. 1, pp. 99-109, 2021, doi: 10.1007/s40031-020-00506-0.
- [15] D. S. Sankaralingam, M. S. N. Balasubramanian and Krishnaveni L, "Performance improvement of Photo-Voltaic panels by Super-Lift Luo converter in standalone application," *Materials Today: Proceedings*, vol. 37, part 2, pp. 1163-1171, 2021, doi: 10.1016/j.matpr.2020.06.352.
- [16] H. A. Sher, A. F. Murtaza, A. Noman, K. E. Addoweesh, K. Al-Haddad and M. Chiaberge, "A New Sensorless Hybrid MPPT Algorithm Based on Fractional Short-Circuit Current Measurement and P&O MPPT," in *IEEE Transactions on Sustainable Energy*, vol. 6, no. 4, pp. 1426-1434, Oct. 2015, doi: 10.1109/TSTE.2015.2438781.
- [17] S. Bhattacharyya, D. S. Kumar P, S. Samanta and S. Mishra, "Steady Output and Fast Tracking MPPT (SOFT-MPPT) for P&O and InC Algorithms," in *IEEE Transactions on Sustainable Energy*, vol. 12, no. 1, pp. 293-302, Jan. 2021, doi: 10.1109/TSTE.2020.2991768.
- [18] R. B. Bollipo, S. Mikkili and P. K. Bonthagorla, "Hybrid, optimal, intelligent and classical PV MPPT techniques: A review," in *CSEE Journal of Power and Energy Systems*, vol. 7, no. 1, pp. 9-33, Jan. 2021, doi: 10.17775/CSEEJPES.2019.02720.
- [19] J. V. Lagudu, G. Vulasala, and S. S. Narayana, "Maximum energy harvesting in solar photovoltaic system using fuzzy logic technique," *International Journal of Ambient Energy*, vol. 42, no. 2, pp. 131-139, 2021, doi: 10.1080/01430750.2018.1525589.
- [20] M. M. Killi and S. Samanta, "An Adaptive Voltage-Sensor-Based MPPT for Photovoltaic Systems with SEPIC Converter Including Steady-State and Drift Analysis," in *IEEE Transactions on Industrial Electronics*, vol. 62, no. 12, pp. 7609-7619, Dec. 2015, doi: 10.1109/TIE.2015.2458298.
- [21] M. A. Husain and A. Tariq, "Transient analysis and selection of perturbation parameters for PV-MPPT implementation". *International Journal of Ambient Energy*, vol. 41, no. 10, pp. 1176-1182, 2020, doi: 10.1080/01430750.2018.1517661.
- [22] M. Kokila, P. Manimekalai and V. Indragandhi, "Design and development of battery management system (BMS) using hybrid multilevel converter," *International Journal of Ambient Energy*, vol. 41, no. 7, pp. 729-737, 2020, doi: 10.1080/01430750.2018.1492440.
- [23] R. Katuri, S. Gorantla, and K. Suresh, "Investigation on intelligent controllers performance used in electric vehicle application," *International Journal of Ambient Energy*, 2020, doi: 10.1080/01430750.2020.1861092.
- [24] P. K. Maroti, S. Padmanaban, J. B. Holm-Nielsen, M. Sagar Bhaskar, M. Meraj and A. Iqbal, "A new structure of high voltage gain SEPIC converter for renewable energy applications," in *IEEE Access*, vol. 7, pp. 89857-89868, 2019, doi: 10.1109/ACCESS.2019.2925564.
- [25] B. Singh and R. Kushwaha, "A PFC based EV battery charger using a bridgeless isolated SEPIC converter," in *IEEE Transactions on Industry Applications*, vol. 56, no. 1, pp. 477-487, Jan.-Feb. 2020, doi: 10.1109/TIA.2019.2951510.

**BIOGRAPHIES OF AUTHORS**

**Dheeban Sembulingam Sankaralingam**    is currently working as an Assistant Professor in the Department of Electrical and Electronics Engineering at Sri Venkateswara College of Engineering Sriperumbudur, Chennai, India. He has completed his Master of Engineering in Power Electronics and Drives from SSN College of Engineering Chennai, Tamilnadu, 2016 with distinction and bachelor of engineering in electrical and electronics engineering from MEPCO Schlenk Engineering College Sivakasi, Tamilnadu, 2014. He can be contacted at email: dheebanss@ieee.org.



**Muthu Selvan Balasubramanian Natarajan**    is currently working as an Associate Professor in the Department of Electrical and Electronics at Sri Sivasubramaniya Nadar College of Engineering and has 15 years of teaching experience which includes 10 years of research experience in the field of power system optimization. He received his B.E (EEE – Distinction) degree (2000) and M.B.A (Finance) degree (2002) from Madurai Kamaraj University. He obtained an M.E. degree (2004) and a Ph.D. degree (2013) in the field of Power System Engineering from Anna University, Chennai. His area of interest includes Power System Optimization, Application of Power Electronics controllers to Power System, Renewable energy system. He can be contacted at email: nbmselvan@gmail.com.



**Maheswari Muthusamy**    is working as an Assistant Professor in the Department of Electrical and Electronics Engineering at AAA College of Engineering and Technology Sivakasi. She received her B.E degree from Kalasalingam Institute of Technology Srivilliputtur (2013) and M.E degree from MEPCO Schlenk Engineering College Sivakasi (2015), Her area of interests includes Power Electronics and Electrical Machines. She is an active member of Institute of Engineers India. She can be contacted at email: maheswari@aaacet.ac.in.



**Sarojini Bagavath Singh**    is working as an Assistant Professor in the Department of Electrical and Electronics Engineering at AAA College of Engineering and Technology Sivakasi. She received her B.E degree from Kamaraj College of Engineering (2009) with Distinction and M.E degree from Anna University Trichy (2013), Her area of interests includes Power Electronics and Drives. She has a vast teaching experience of 11 years. She can be contacted at email: sarojini@aaacet.ac.in.